JOURNAL OF AGRICULTURAL AND FOOD CHEMISTRY

Multi-Level Approach for the Analysis of Water Effects in Corn Flakes

ABEL E. FARRONI,*,†,‡ SILVIA B. MATIACEVICH,† SANDRA GUERRERO,† STELLA ALZAMORA,† AND M. DEL PILAR BUERA†

Departamento de Industrias, Facultad de Ciencias Exactas y Naturales, Universidad de Buenos Aires, C1428EGA Buenos Aires, Argentina, and Laboratorio de Calidad de Alimentos EEA Pergamino, INTA Av. Frondizi (Ruta 32) Km 4, 5 Pergamino, Buenos Aires, Argentina CC 31-B2700WAA

The purpose of this work was to analyze the effect of water on thermal transitions, mechanical properties, and molecular mobility in corn flakes (CF), and their relationships. Commercial common (CCF) and sugar-frosted (SCF) corn flakes were studied in a water content (wc) range from 5 to 20 (% dry basis). The slope of ^{1}H NMR spin−spin relaxation time T_2* (determined by FID) versus temperature plot changed close to T_g. Compression force showed a maximum at wc of ca. 12 and 16% (db) for SCF and CCF, respectively. ^{1}H NMR complemented DSC data in determining the temperature dependence of water and solid mobility, in order to assess quality of laminated corn products. The results of the present work indicate that while the compression force showed a maximum value as a function of water content, T_g values determined by DSC or by spin−spin relaxation decreased progressively with increasing water content.

KEYWORDS: Corn flakes; texture; water mobility; ^{1}H NMR, DSC

INTRODUCTION

The shelf stability and textural properties of food products are closely related to their mechanical and thermal properties. The physical state, water mobility, and water−solid interactions affect storage stability, textural, and functional properties of food. Crispiness and crunchiness are sensations related to the fracture properties of food materials, and they are the most important characteristics that define customer preference in snacks. The distinction between crispy and crunchy behavior is not very clear since the definitions varied between different studies and likely between different countries and products (*1*). For the evaluation of crispy products, a single fracture event may serve well, but certainly for crunchy behavior, a more complex fracture pattern is required, consisting of a series of successive fracture events. In previous works on breakfast cereals, the term crispness was used to describe fracture behavior (*2–4*). It has been reported that crispness is highly sensitive to moisture change (*5–7*). If the moisture of products increases due to water sorption from the atmosphere (which depends on the specific food material) or by mass transport from neighboring areas, the plasticizing effect of water severely reduces crispness (*5*). Loss of crispness occurs when moisture content of the product exceeds the monolayer moisture content (*6, 8*). The behavior associated with crispness has been shown to be associated with the glassy state, implying the onset of molecular motion below the glass transition temperature (T_g) (*9*). Decrease of mechanical resistance with increasing water amounts in cereal-based products emphasized the plasticizing effect of water, reducing T_g (*3, 10*). However, the prediction of crispness, on the basis of knowledge of the glass transition temperature alone, was not possible, because biopolymers can exhibit different fracture mechanisms in the glassy state. Water influences the rheological properties of food in liquid and solid states alike. In solid foods, water affects their response to force. Increasing water content can lead to plasticizing or antiplasticizing effects (*11*). The plasticization of polymer chains facilitates deformation, and brittle material becomes softer and loses crispness. The mechanism of the antiplasticizing effect of water is not fully understood. Harris and Peleg (*12*) suggested that water adsorbed by glass could make the matrix more compact and increase its resistance to deformation. However, Fontanet et al. (*13*) claimed that water causes the rearrangement of biopolymers in glass, and a more cohesive structure is formed. Chang et al. (*14*) proposed a hole-filling mechanism involving the filling of holes created under high stress with the diluent's molecules. Texture in breakfast cereals was shown to be influenced by the mechanical properties of their constitutive materials, grain features, and the applied industrial processes (*3*). In corn starch-zein blend model systems, mechanical properties were affected by adhesion of the constitutive materials and phase separation (*15*). The corn flake lamination process produces important changes in corn endosperm components: starch is gelatinized, protein bodies are disrupted, and zeins are partially released and form extensive disulfide bond crossover (*16*). In this way, the interaction between process and material

* To whom correspondence should be addressed. Phone: 54 11 4576 3397. Fax: 54 11 4576 3366. E-mail: afarroni@pergamino.inta.gov.ar.
† Universidad de Buenos Aires.
‡ Laboratorio de Calidad de Alimentos EEA Pergamino.

10.1021/jf800541f CCC: $40.75
Published on Web 07/11/2008

properties are of major importance in the building of structure and determination of texture. Although sensory analysis gives the complete description of texture, there has been a great interest in developing instrumental techniques to assess crispness (*4*). Lewicki et al. (*11*) studied the texture properties of crispy bread as a function of water content using the compression test. They observed antiplasticizing effects of water between 3 and 9%; then, up to 11%, there was an apparent hardening of the material. Beyond 11% of water content, the apparent stiffness modules decreased and the softening effect of water became dominant, and an antiplasticizing effect is observed. Water molecules in biological materials may have different mobility according to their degree of interaction with solids (*17*). Low moisture products remain brittle in the glassy state, which can be studied by differential scanning calorimetry (DSC) (*18*). Molecular mobility can be considered from a structural and macromolecular level, and therefore, T_g can be a descriptive parameter of the physical state of macromolecules, which differs from the molecular mobility of smaller molecules such as water (*19*). As polymers adsorb water, their properties are not affected in the same manner, and in the low to intermediate humidity range, some mechanical properties show a maximum when plotted versus water content while T_g continuously decreases (*14*). Proton nuclear magnetic resonance (^{1}H NMR) transversal relaxation times (T_2) provide useful information on molecular mobility and water populations as being affected by the water−solid interactions (*20*). ^{1}H NMR allows one to assess differences in molecular mobility on polymers by measuring the changes in spin−spin (T_2) or spin−latice (T_1) relaxation constants with temperature or water content (*21*).

The purpose of this work was to compare the effect of water content on supramolecular thermal and mechanical properties of corn flakes (CF) and their relationship with molecular mobility.

MATERIALS AND METHODS

Samples. Commercial corn flakes, common (CCF), and sugar-frosted corn flakes (SCF) were provided by the manufacturer shortly after processing. Corn flakes were made by the gelatinization lamination process. Briefly, the process implies batch steam cooking of flaking grits (endosperm fragments), cooling, and tempering, lamination, and toasting. To produce the sugar frosted surface, common corn flakes are coated by spraying a sucrose solution and dried. During this last step, sucrose crystallization occurs on the surface of the flakes. Composition data (provided by the manufacturer) of SCF and CCF samples were total sugar content (36%, 6.1%), proteins (5.2%, 6.6%), lipids (0.7%, 1.0%), and fiber (2.6%, 3.2%), and available carbohydrates were 85% for both samples.

Water Content and Relative Vapor Pressure. In order to achieve different water content, samples were put into vacuum desiccators for 20 days at 25 °C, employing saturated salt solutions at relative vapor pressures (RVPs) in the range between 11 and 80% (*22*). The salt solutions used were LiCl (RVP 11%), $MgCl_2$ (RVP 33%), K_2CO_3 (RVP 44%), NaCl (RVP 75%), and KCl (RVP 84%). No special care was taken about microbial growth below or at 75% RVP. After about 20 days at a RVP of 84%, microbial growth was observed, and the corresponding samples were discarded. Accordingly, none of the analyzed samples presented any evidence of fungal growth during storage upon examination with an ocular stereoscope (Unitron MS, NY).

After 20 days, the RVPs of the systems were determined by dew point using an Aqualab Series 3 (Decagon Devices, Pullman, Washington, USA), and water content (wc) was determined gravimetrically by difference in mass before and after drying the samples in an oven at 105 °C to constant weight (*23*). Results were expressed as percentage in dry basis (% db). Water adsorption data were fitted to the Guggenheim−Anderson−de Boer (GAB) equation, which is the most widely employed model in food systems since it applies over a wide range of RVP (*24*).

The GAB constants m_0, C, and k were obtained by transforming the GAB equation to the quadratic form:

$$\frac{a_w}{m} = \left(\frac{1}{m_0 Ck}\right) + \left(1 - \frac{2}{C}\right)a_w + \left(\frac{(1/C) - 1}{m_0}k\right)a_w^2 \qquad (1)$$

where m is the water content in dry basis, a_w is the water activity measured as relative vapor pressure divided by 100, m_0 is the GAB monolayer water content, C is the Guggenheim constant that is related to the heat of sorption of the first layer on primary sites, and k is a factor correcting the properties of the multilayer molecules with respect to the bulk liquid. C and k are related to the energy of interaction between mono- and multilayer water molecules, and they reflect the temperature effect on sorption properties. k is practically without exception close to but less than unity. The quality of the GAB model fit was assessed from the value of the relative percent deviations of predicted water content values (% E) (*24*).

Mechanical Properties. Mechanical properties were measured by a compression test, employing a model 1011 universal testing machine (Instron, Canton, Massachussets, USA) equipped with a 35 mm diameter piston. In each assay, the weight of corn flakes varied between aproximately 10 and 12 g, depending on water activity. Thirty millimeter thick beds of corn flakes were compressed in a 50 mm diameter cylinder up to a fixed 30% deformation, using the piston at 50 mm/min velocity. The percent deformation used was selected according to those reported by other authors for these types of samples (*5, 25*). The force at maximum deformation was measured at the point piston stop. Five to eight replicates were measured for each sample according to sample availability. Grubbs' test was used to detect outliers, which were removed from the data set, then replicates were averaged (*26*). Force versus distance plots were obtained, recording the initial point in the curve as the compression force higher than 0.01 kg; smaller force values are considered noise. In order to quantify curve jaggedness, the plots were fitted for different curves, and analysis of variance and of residuals were performed. Third order polynomial on one variable was considered the best model and was chosen for the jaggedness analysis, according to eq 2 (*27*).

$$y = a + bx + cx^2 + dx^3 \qquad (2)$$

where y = force (F); x = distance (d); a, b, c, and d = model parameters.

The dispersion of residuals was used as a measure of curve jaggedness (*7*). Prism 4 software (GraphPad Software, Inc. San Diego, USA) was employed for these calculations.

Thermal Transitions. Approximately 15 mg of ground samples were weighed with a precision of ± 0.01 mg, sealed into aluminum pans (40 μL capacity), and loaded into a model 822 differential scanning calorimeter (DSC) (Mettler Toledo, Schwerzenbach, Switzerland). Heat flux was measured with a resolution better than 0.04 μW. All experiments were performed in duplicate following the same protocol. The instrument was calibrated using indium, zinc, and lead. An empty pan was used as reference. The DSC thermograms were obtained from −50 to 150 °C at a heating rate of 10 °C/min. This heating rate is commonly selected in order to clearly observe biopolymer transitions (*28–30*). The glass transition temperature (T_g) was determined as the onset temperature of the discontinuities in heat flow versus temperature curves (indicating a change in specific heat). All thermograms were analyzed using STAR^e Software v. 6.1 (Mettler Thermal Analysis).

Molecular Mobility. Time-resolved proton nuclear magnetic resonance (^{1}H NMR) measuring the spin−spin transverse relaxation times (T_2) were used to determine water and solid mobility. A pulsed nuclear magnetic resonance (^{1}H NMR) Bruker Minispec spectrometer model mq 20 (Bruker Biospin GmbH, Rheinstetten, Germany), with a 0.47 T magnetic field operating at resonance frequency of 20 MHz and thermostatted at 40 °C, was used for the measurements. The spin−spin relaxation times obtained from free induction decay (FID) following a single 90° pulse is affected by field inhomogenities. Nuclei in one part of the sample will experience a magnetic field slightly different from that experienced by identical nuclei in another region. This apparent

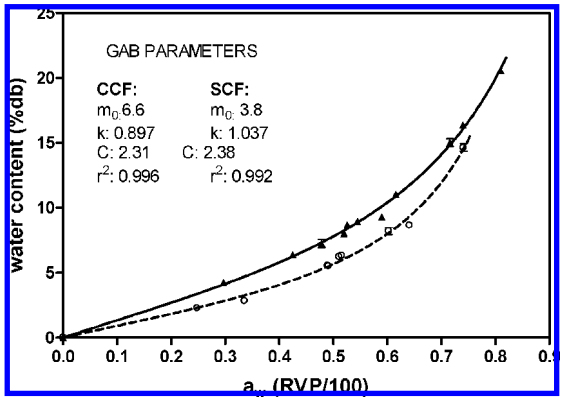

Figure 1. Water content vs RVP plot for CCF (▲) and SCF (○) fitted to the GAB equation. The error bars represent standard deviation.

relaxation time is designated T_2*. Only the relaxation times of fast relaxing protons (which are in the microsecond range) can be correctly measured without a 180° refocus pulse (*31*). In solid samples (like ours), we can consider that the intrinsic T_2 is very close to T_2*, as reported previously by Fullerton and Cameron (*17*). FID analysis was used to evaluate proton mobility associated with the solid matrix in the range 4−90 °C (*10*). Ground samples were placed in 10 mm diameter glass tubes (to 5 cm height) and equilibrated at different temperatures (from 5.0 to 90.0 °C) in a thermostatted bath (Thermo Haake C35P, Germany) before measuring T_2*. The FID test itself if very fast, taking 10 s, and samples could be measured without appreciable temperature modification. The decay envelopes were fitted to monoexponential behavior with the following equation:

$$I = A^{-t/T_{2FID}} \quad (3)$$

where I represents proton signal intensity, T_{2FID} corresponds to the relaxation time (T_2*) of protons in the polymeric chains of the sample and tightly bound water, and A is a constant.

Longer relaxation times (such as those corresponding to more mobile protons) can be measured after a refocusing pulse. In order to obtain information on the T_2 values of the slow relaxing protons, the Hahn spin−echo pulse sequence (90°−τ−180°) with an interpulse (τ) range of 0.001−4 ms was used. The interpulse range was selected to allow for registering of the complete decay of the signal. The decay envelopes were fitted to biexponential behavior with the following equation:

$$I = A_1^{(-t/T_{2S})} + A_2^{(-t/T_{2L})} \quad (4)$$

where I represents the ^{1}H NMR signal intensity at time t. The relaxation time T_{2S} corresponds to the protons in the less mobile water fraction. A_1 is proportional to the number of protons in the T_{2S} state. The relaxation time T_{2L} corresponds to the more mobile water fraction. A_2 is proportional to the number of protons in the T_{2L} state.

RESULTS AND DISCUSSION

As shown in **Figure 1**, common corn flakes showed higher water content than sugar frosted flakes at the same RVP. This result was attributed to the presence of crystalline sucrose deposited on the surface of the flakes. Sucrose crystals are very ordered structures and sorb very little water until water activity reaches approximately 0.8 and sucrose starts to dissolve (*32*). The GAB model equation (*12*), allowed for the description of the water content of the different samples in the whole range of studied RVPs. The GAB parameters (m_o, k, and C) for both types of corn flakes samples are also shown in **Figure 1**. The correlation coefficients (r^2) obtained were 0.996 and 0.992 for CCF and SCF, respectively, and the relative percent deviations of predicted water content values (% E) were 2.8 for the common corn flake curve and 5.4 for sugar frosted, reflecting a good predictive value of the parameters obtained. The constant

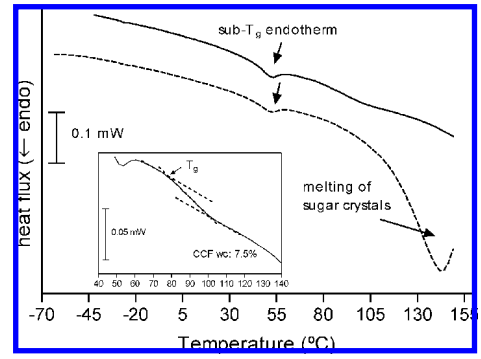

Figure 2. DSC thermograms of CCF (—) and SCF (---) at 7.5% (db) and 5.2% (db) water content (wc), respectively. Main transitions are shown with arrows. The inset shows the glass transition in CCF.

k for the analyzed materials was lower (CCF) or very close (SCF) to unity, as it is in many food materials (*33*).

Figure 2 shows the DSC thermograms obtained for CCF and SFC at water content of 7.0% and 5.0% in dry basis, respectively. The endothermic event observed close to 50 °C disappeared on an immediate rescan. However, it reappeared after aging the samples for 2 days at 25 °C. This event was previously described as a sub-T_g endotherm in starch-containing systems (*34*) since it occurs at temperatures below T_g. The glass transition temperatures of CCF decreased at increasing water content, as expected, and were slightly lower than values previously reported for gelatinized corn starch (*35*). The main components in corn flakes, which determine the characteristic structure and thermal transitions, are gelatinized starch and proteins. Lipids and sugars, in a lower amount could influence structure and the thermal transitions as well. Thus, the difference of T_g values in corn flake with those of gelatinized starch accounts for the presence of those components. In SCF samples, endothermal transition starts at 70 °C, showing a peak close to 147 °C, as shown in **Figure 2**. On the basis of previous literature data (*36*), the transition was attributed to melting of sugar crystals and simultaneous caramelization, which was evidenced by the browned appearance of the samples when opening the DSC pan after the runs. The addition of crystalline sucrose to common corn flakes (in a proportion similar to that in sugar-frosted corn flakes) promoted similar DSC thermograms than frosted corn flakes (data not shown).

In sugar frosted samples, T_g was not detectable because it was overlapped by the described thermal events (sub-T_g endothermal peak or caramelization reaction).

The study of ^{1}H NMR spin−spin transverse relaxation times (T_2) as a function of water content and temperature provides information about the mobility of protons belonging to water and/or solids, according to the pulse sequence employed. **Figure 3** (**A** and **B**) shows the T_2* values obtained by free induction decay analysis (T_{2FID}) for common (**A**) and sugar frosted (**B**) corn flakes at different water content as a function of temperature. When a single 90° pulse was employed, the T_{2FID} value increased with increasing water content and temperature, reflecting higher mobility of the protons in solids (*37*) and in water molecules, strongly interacting with them. In common corn flake samples corresponding to water content of 11.0% and 16.4%, a change of slope in the T_{2FID} versus temperature was observed. This event occurred at a temperature value that was close to the T_g value determined by DSC. This change of slope could be detected in samples in which the T_g value was in the available range of experimental temperatures (5 to 80 °C). For samples with lower water content, glass transition temperatures were too high to be detected in this experiment

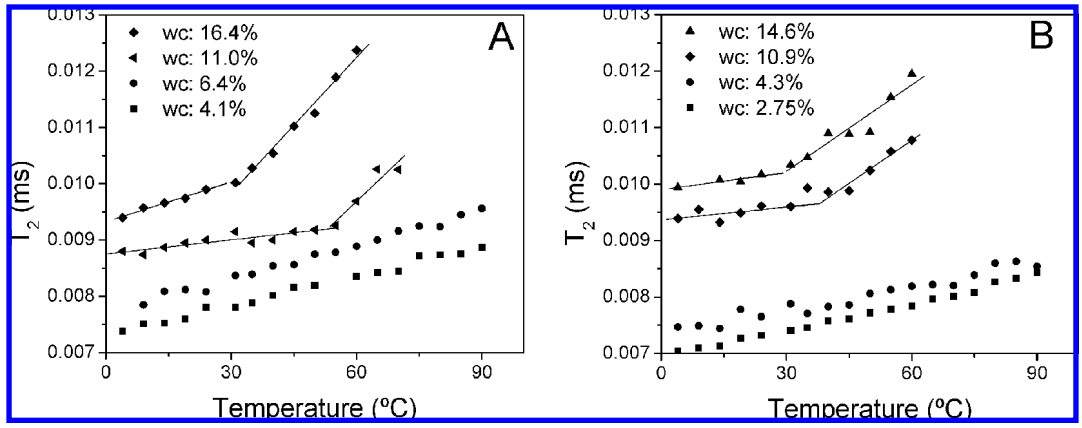

Figure 3. Relationship between T_{2FID} and temperature for common corn flakes (**A**) and sugar-frosted corn flakes (**B**) for different water content. A change of slope was observed at a temperature value close to T_g determined by DSC at the same water content.

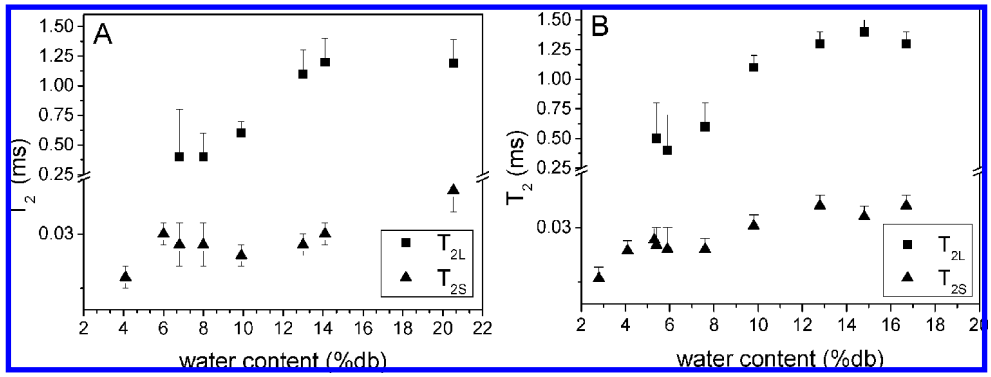

Figure 4. T_2 vs water content for CCF (**A**) and SCF (**B**). The error bars represent standard deviation. Two sets of T_2 values were obtained using a Hahn spin−echo sequence. A short relaxation time cluster was defined as T_{2S} (π). The longer relaxation times (characteristic of more mobile protons, such as those of bulk water) were assigned as T_{2L} (■).

without appreciable water evaporation. In the more complex sugar frosted systems (**Figure 3B**), a change of slope was less marked than in CCF, but still could be detected. Probably adding additional components such as sugar makes transitions broader and more difficult to define because of the contribution of each component, which has its own transition temperature, to the global transition of the system. As discussed before, T_g values could not be determined in sugar frosted corn flakes by DSC, and the comparison with T_{2FID} measurements was not possible. A nonzero slope in the T_{2FID} versus temperature plot before the transition indicated that mobility existed even before the glass transition occurred (*21*). As shown in **Figure 3** (**A** and **B**), CCF samples showed a higher positive slope than SCF in the temperature region below T_g, which indicates that as temperature increased, proton mobility increased faster in CCF samples than in SCF samples. As a consequence of their connection with molecular mobility, Lin et al. (*21*) have related the slopes of the T_{2FID} versus temperature curves below T_g with the rate of product quality changes during storage. According to this, common corn flakes are expected to manifest more changes below T_g than sugar frosted ones.

The spin−spin time relaxation, T_2, evaluated using a Hahn spin−echo sequence allows the measurement of proton magnetic relaxations characterized by higher T_2 values than those determined by FID. These populations are affected by field inhomogenities, and a refocus pulse is needed to obtain an accurate measurement. In this way, this spin−echo pulse sequence can be used to differentiate proton populations with different mobility as a function of water content and to study the relaxation of water protons occurring after the protons corresponding to solids have relaxed. Two sets of T_2 values were obtained after the spin−echo sequence, which were related to solids and water populations displaying different degrees of interaction with solids. As in the case of T_{2FID}, the short relaxation times, T_{2S}, were attributed to solids and water molecules displaying stronger interactions with solids. (T_{2S} is different from T_{2FID} because of the different technique employed.) The higher relaxation time constant was assigned as T_{2L} and corresponds to proton populations with higher mobility and therefore less interaction with solids. These proton populations were previously described (*38, 39*). In both types of systems, (**Figure 4A** and **B**) the Hahn spin−echo analysis showed that only the rapidly relaxing proton population with T_{2S} values at 25−30 μs was present at water content up to 6.5% or 5.0% (db) for CCF and SCF, respectively, which were close to the GAB monolayer value (m_o). A slight change in the T_{2S} versus water content slope was observed at a water content (ca. 13.5% in common corn flakes) at which the T_g values of the samples were about the NMR measurement cell temperature (40 °C). This change of T_2 versus wc dependence reflected an increased proton mobility with increasing water content, but was less pronounced than the temperature dependence observed for T_{2FID}. The increased relaxation time with increasing water content for the more mobile proton populations has been observed by other authors, for example, Acevedo et al. (*40*). At water content values above m_o, calculated by the GAB equation, a slowly relaxing component was observed (T_{2L}), whose relaxation constant increased with increasing water content in the range between 0.4 and 2.5 ms. The intensity of the NMR signal corresponding to a particular proton population offers a relative estimation of the amount of protons contributing to those T_2 values. In the case of T_{2L} (attributed to water protons

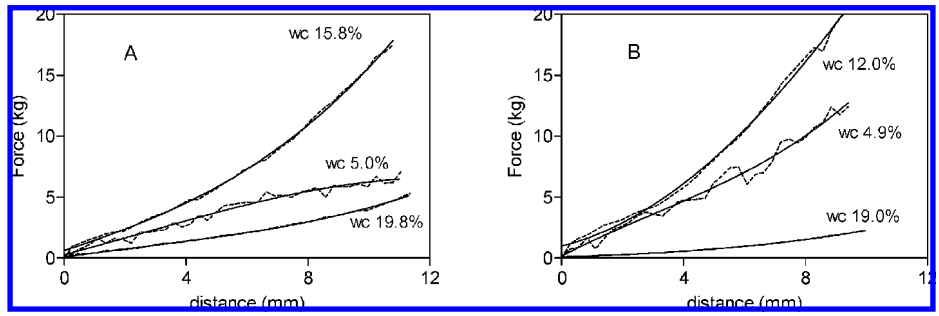

Figure 5. Compression curves (···) and fitted curve (—) according to eq 1 for CCF (**A**) and SCF (**B**) at different water content.

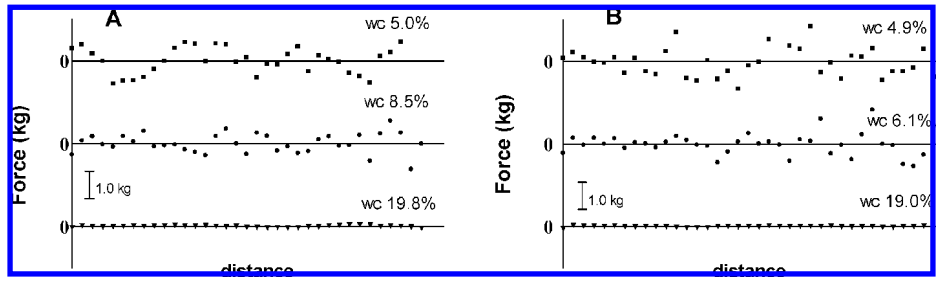

Figure 6. Fit residuals from force deformation curves for different water content in CCF (**A**) and SCF (**B**).

with higher mobility), the signal intensity increased with water content, indicating the increase in water molecules contributing to it (data not shown). At water content above 20% for CCF (**Figure 4A**), T_{2L} tends to reach a plateau, as described previously by Ablett et al. (*28*) and Acevedo et al. (*40*).

Changes in mechanical properties in response to compression were studied at different water content. A third order polynomial model was fitted to compression curves to quantitatively evaluate how its irregularity was affected by water content. The dispersion of residuals was used as a measure of curve jaggedness. As the water content of both types of corn flakes increased, compression curves became smoother and less serrated, and thus, the mathematical fit was better (**Figure 5**). The determination coefficient (r^2) fluctuated between 95% (CCF) and 97% (SCF) for low wc samples and increased to 99.9% for both kinds of corn flakes.

Figure 6 shows the change in fit residuals from force deformation curves for different water content: CCF (**Figure 6B**) and SCF (**Figure 6B**). In order to better appreciate the graph, only three water contents of each type of corn flakes are plotted. Corn flakes are cellular solids, that is, they have a porous structure consisting of a solid matrix surrounding air cells (*3, 7*). Crunchy cellular solid foods are difficult to deform but break relatively easily. Mechanical behavior as function of water content for this type of materials has been clearly explained by Luyten et al. (*1*). At very low water content, corn flakes behaved as a brittle material, and the fracture strain was small. Fracture behavior consisted of a series of successive fracture events involving repetitive deformation and fracture of subsequent layers in the product. In this way, as corn flakes in the cylinder were compressed, the increase in force was accompanied by different fracture events. Each fracture event went along with a drop in force. Further loading caused the force to increase again (*1*). As compression proceeded, broken fragments rearrange, occupying empty spaces, and the sample became compacted and more difficult to compress. At water content higher than 8.5% (db) for CCF and 6% db for SCF, the residual dispersion decreased sharply in conjunction with smoother deformation curves. The loss of jaggedness indicated the change in the mechanics of compression: at low water content, brittle fracture predominates, while at high water

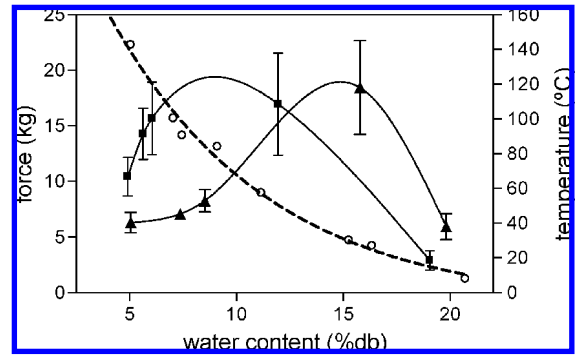

Figure 7. Force at maximum deformation for CCF (π) and SCF (■), and onset temperature of glass transition for CCF (○) at different water content. Symbols represent experimental values. Solid lines are the results of spline fit indicating the tendency of data points. The error bars represents standard deviation.

content, plastic deformation and wrinkling of intact air cell walls occurs (*41*). The smoothing of deformation curves begins while the material is in the glassy state, indicating that mechanisms other than the overall physical state of the system are involved (as discussed in refs *2, 15, and 42*).

Force at maximum deformation showed a particular behavior when analyzed at different water content (**Figure 7**). At low water content, the force for sugar frosted flakes was higher than common corn flakes. Then the force increased as water content increased for both types of samples, indicating an antiplasticizing effect of water (*7*). This effect was more pronounced for SCF samples, which showed a very steep increase of force values with increasing water content in the low wc region. A previous work (*42*) showed opposite results for sensory crispness and deformation force in model systems composed of waxy maize starch and sucrose. In these systems, sucrose and starch were mixed in an aqueous suspension before extruding. Thus, in these systems the sugar must have remained amorphous, integrated in the whole dough, which is not the case in sugar frosted corn flakes, in which the sugar is crystallized on the surface of the flakes. Sugar crystal coating adds an additional layer of material to corn flakes, and, before water starts to dissolve those crystals, it may present additional resistance to compression. This could

explain the difference in stiffness between CCF and SCF. It is interesting to note that the slope of the T_{2FID} versus temperature curves below T_g, related to proton mobility in the glassy state, was more marked for CCF as shown in **Figure 4**, and consequently, the higher antiplasticizing effect observed in the compression test for SCF samples (as shown in **Figure 7**) could be related to the lower molecular mobility in SCF samples (*21*). Lewicky et al. (*11*) observed that the response to force deformation in solid foods was affected by increasing water content and can lead to plasticizing or antiplasticizing effects. Partanen et al. (*43*) observed a decrease in molecular motion in amylose films induced by glycerol and evidenced by longer H NMR T_1 relaxation times at temperatures below T_g. This effect was related to an antiplasticizing effect of glycerol, and with a further water or glycerol content increase, the plasticizing effect became evident.

The results of present work indicate that while the compression force showed a maximum as a function of water content (antiplasticizing effect), the glass transition temperatures decreased progressively with increasing water content, which is the expected behavior for T_g. As water content increased starting from far below T_g, covalent bonds in the backbone and side chains of biopolymers show low displacement vibrational movements causing an increase in energy dissipation during deformation at very low water content below T_g. Accordingly, a decrease in fracture speed, an increase in total energy required for deformation, and an increase in required stress were observed (*1*). When the water content reached a critical level, the force of compression decreased. As water content further increased, the mobility of water molecules increased, and plasticizing effects became evident in mechanical properties. When samples were at temperatures close to and above the glass transition temperature, thermal and mechanical properties showed coupled behavior (plasticizing effect). Thus, water plasticizing effect was manifested as a decreased mechanical resistance from critical moisture content. It is to be noted that although the effect of decreasing T_g has often been referred to as the plasticizing effect of water, it is really in the mechanical properties that this effect is manifested. Molecular mobility of small molecules, like water, is determined by local viscosity (at a molecular level) instead of global viscosity (related to glass transition) (*44*). In this way, water may fill inter and intramolecular cavities, acting as an antiplasticizer, according to the observed mechanical behavior (*14*). Previously, Harris and Peleg (*12*) suggested that water adsorbed by glass could make the matrix more compact and increase its resistance to deformation. As shown in the present work, at water content higher than 8.5% for CCF, compression curves showed less fluctuations, reflecting a decrease in brittle fracture.

Both thermal and mechanical transitions occur at the supramomolecular level, they originate from different phenomena, and they are induced by different ranges of perturbation frequencies. In this way, thermal and mechanical properties of corn flakes showed different behaviors as a function of water content. The jaggedness of compression curves was affected by water content below glass transition, indicating a change in sample texture. The T_{2FID} behavior analysis indicated that the samples of SCF, compared to CCF, presented lower proton mobility in the glassy state and that they were the ones that showed a more pronounced antiplasticizing effect in the low water content region. In spite of the proved mobility of water in the glassy state (*28*), the higher antiplasticizing effect and decreased proton mobility observed in SCF samples may be a consequence of the ability of water to act as a filler in small cavities, enhanced by the sugar component in these samples. Thus, ^{1}H NMR, which provided data of motions at the molecular level, could facilitate the interpretation of thermal and mechanical properties, depending on supramolecular interactions that are relevant in assessing the quality of laminated corn products.

ACKNOWLEDGMENT

We thank Dr. Miryan Cassanello for valuable advice on data analysis.

LITERATURE CITED

(1) Luyten, H.; Plijter, J.; Van Vliet, T. Crispy/crunchy crusts of cellular solid foods: a literature review with discussion. *J. Text. Stud.* **2004**, *35*, 445–492.
(2) Chaunier, L.; Courcoux, P.; Della Valle, G.; Lourdin, D. Physical and sensory evaluation of corn flake crispness. *J. Text. Stud.* **2005**, *36*, 93–118.
(3) Chaunier, L.; Della Valle, G.; Lourdin, D. Relationships between texture, mechanical properties and structure of cornflakes. *Food Res. Int.* **2007**, *40*, 493–503.
(4) Roudaut, G.; Dacremont, C.; Vallès Pàmies, B.; Colas, B.; Le Meste, M. Crispness: a critical review on sensory and material science approaches. *Trends Food Sci. Technol.* **2002**, *13*, 217–227.
(5) Suwonsichon, T.; Peleg, M. Instrumental and sensory detection of simultaneous brittleness loss and moisture toughening in three puffed cereals. *J. Text. Stud.* **1998**, *29*, 255–274.
(6) Li, Y,.; Kloeppel, K.; Hsieh, F. Texture of Glassy Corn Cakes as a Function of Moisture Content. *J. Food Sci.* **1998**, *63*, 869–872.
(7) Gondek, E.; Lewicki, P. Antiplasticization of cereal-based products by water. Part II: Breakfast cereals. *J. Food Eng.* **2006**, *77*, 644–652.
(8) Katz, E.; Labuza, T. Effect of water activity on the sensory crispness and mechanical deformation of snack food products. *J. Food Sci.* **1981**, *46*, 403–409.
(9) Nicholls, R.; Appelqvist, A.; Davies, A.; Ingman, S.; Lillford, P. Glass transition and fracture behaviour of gluten and starches within the glassy state. *J. Cereal Sci.* **1995**, *21*, 25–36.
(10) Roudaut, C.; Dacremont; Le Meste, M. Influence of water on the crispness of cereal-based foods: acoustic, mechanical, and sensory studies. *J. Text. Stud.* **1998**, *29*, 199–213.
(11) Lewicki, P.; Jakubczyk1, E.; Marzec, A.; Carmo Cabral, m.; Pereira, P. Effect of water activity on mechanical properties of dry cereal products. *Acta Agrophysica* **2004**, *4*, 381–391.
(12) Harris, M.; Peleg, M. Patterns of textural changes in brittle cellular foods caused by moisture sorption. *Cereal Chem.* **1996**, *73*, 225–231.
(13) Fontanet, I.; Davidou, S.; Dacremont, C.; Le Meste, M. Effect of water on the mechanical behaviour of extruded flat bread. *J. Cereal Sci.* **1997**, *25*, 303–311.
(14) Chang, Y.; Cheah, P.; Seow, C. Plasticizing-antiplasticizing effects of water on physical properties of tapioca starch films in the glassy state. *J. Food Sci.* **2000**, *65*, 445–451.
(15) Chanvrier, H.; Della Valle, G.; Lourdin, D. Mechanical behavior of corn flour and starch zein based materials in the glassy state: A matrix-particle interpretation. *Carbohydr. Polym.* **2006**, *65*, 356–356.
(16) Batterman-Azcona, S.; Hamaker, B. Changes occurring in protein body structure and α-zein during cornflake processing. *Cereal Chem.* **1998**, *75*, 217–221.
(17) Fullenton, G.; Cameron, I. Relaxation of Biological Tissues. In *Biomedical Magnetic Resonance Imaging: Principles, Methodology, and Application*; Wehrli, F. W., Kneeland, J. B., Eds.; VCH Inc.: New York, 1988; p 115.
(18) Slade, L.; Levine, H. Water and the glass transition-dependence of the glass transition and chemical structure: Special implication for flour functionality on cookie baking. *J. Food Eng.* **1995**, *22*, 143–188.

(19) Vittadini, E.; Chinachoti, P. Effect of physico-chemical and molecular mobility parameters on *Staphylococcus aureus* growth. *J. Food Sci. Technol.* **2003**, *38*, 841–847.
(20) Kou, Y.; Dickinson, L. C.; Chinachoti, P. Mobility characterization of waxy corn starch using wide-line ^{1}H nuclear magnetic resonance. *J. Agric. Food Chem.* **2000**, *48*, 5489–5495.
(21) Lin, X.; Ruan, R.; Chen, P.; Chung, M.; Ye, X.; Yang, T.; Doona, C.; Wagner, T. NMR state diagram concept. *J. Food Sci.* **2006**, *71*, R136−R145.
(22) Greenspan, L. Humidity fixed points of binary saturated aqueous solutions. *J. Res. Natl. Bur. Stand.* **1977**, *81*, 89–96.
(23) American Association of Cereal Chemists. *Approved Methods of the A ACC*, 9th ed.; The Association: St. Paul, MN, 1995; pp 44−16.
(24) Lomauro, C.; Bakshi, A.; Labuza, T. Evaluation of food sorption isotherms equations, I: Fruit, vegetable and meat products. *Lebensn.-Wiss. Technol.* **1985**, *18*, 111–117.
(25) Peleg, M. Mechanical Properties of Dry Brittle Cereal Products. In *The Properties of Water in Foods*; Reid, E., Ed.; CRC Press: London, UK, 1998; pp 233−253.
(26) Stefanzky, W. Rejecting outliers in factorial designs. *Technometrics* **1972**, *25*, 30.
(27) Henry, Z.; Zhang, H.; Onks, D. New model for elastic behaviour of cellular material. *J. Agric. Eng. Res.* **2000**, *76*, 399–408.
(28) Ablett, S.; Darke, A.; Izzard, M.; Lillford, P. Studies of the Glass Transition in Malto-Oligomers. In *The Glassy State of Foods*; Blanshard, J., Lillford, P., Eds.; Nottingham University Press: Loghborough, Leicestershire, UK, 1993; pp 189−206.
(29) Sopade, P.; Halley, P.; Junmingb, L. Gelatinisation of starch in mixtures of sugars. II. Application of differential scanning Calorimetry. *Carbohydr. Polym.* **2004**, *58*, 311–321.
(30) Tananuwong, K.; Reid, D. Differential scanning calorimetry study of glass transition in frozen starch gels. *J. Agric. Food Chem.* **2004**, *52*, 4308–4317.
(31) Colquhoun I. Goodfellow B. Nuclear Magnetic Resonance Spectroscopy. In *Spectroscopic Techniques for Food Analysis*; Reiginald, W., Ed.; VCH Publishers Inc: New York, 1994; pp 87−145.
(32) Karel, M. Physico-Chemical Modification of the State of Water in Foods- A Speculative Survey. In *Water Relations of Foods*; Duckworth, R., Ed.; Academic press: New York, 1975; pp 639−657.
(33) Timmermann, E. Multilayer sorption parameters: BET or GAB values. *Colloids Surf., A* **2003**, *220*, 235–260.
(34) Thiewes, H.; Steeneken, P. The glass transition and the sub-T_g endotherm of amorphous and native potato starch at low moisture content. *Carbohydr. Polym.* **1997**, *32*, 123–130.
(35) Zhon, Z.; Sun, S. Thermal characterization and phase behavior of corn starch studied by differential scanning calorimetry. *J. Food Eng.* **2005**, *69*, 453–459.
(36) Bhandari, B.; Roos, Y. Dissolution of sucrose crystals in the anhydrous sorbitol melt. *Carbohydr. Res.* **2003**, *338*, 361–367.
(37) Ruan, R.; Long, Z.; Song, A.; Chen, P. Determination of glass transition temperature of food polymers using low field NMR. *Lebensm.-Wiss. Technol.* **1998**, *31*, 516–521.
(38) Chen, P.; Long, Z.; Ruan, R.; Labuza, T. Nuclear magnetic resonance studies of water mobility in bread during storage. *Lebensm.-Wiss. Technol.* **1997**, *30*, 178–183.
(39) Choi, S.; Kerr, W. ^{1}H NMR studies of molecular mobility in wheat starch. *Food Res. Int.* **2003**, *36*, 341–348.
(40) Acevedo, N.; Schebor, C.; Buera, M. Non-enzymatic browning kinetics analyzed through water-solids interactions and water mobility in dehydrated potato. *Food Chem.* **2008**, *108*, 900–906.
(41) Nuebel, N.; Peleg, M. Compressive stress-strain relationships of two puffed cereals in bulk. *J. Food Sci.* **1993**, *6*, 1356–1374.
(42) Valles Pamies, B.; Rodaut, G.; Dacremont, C.; Le Meste, M.; Mitchell, J. Understanding the texture of low moisture cereal products: mechanical and sensory measurements of crispness. *J. Sci. Food Agric.* **2000**, *80*, 1679–1685.
(43) Partanen, R.; Marieb, V.; MacNaughtanb, W.; Forssell, P.; Farhat, I. ^{1}H NMR study of amylose films plasticized by glycerol and water. *Carbohydr. Polym.* **2004**, *56*, 147–155.
(44) Chinachotti, P. Water Migration and Food Storage Stability. In *Food Storage Stability*; Taub, I., Singh, R., Eds.; CRC Press: Boca Raton, FL, 1997; pp 245−267.

Received for review February 21, 2008. Revised manuscript received May 2, 2008. Accepted May 2, 2008. We acknowledge the financial support of Agencia Nacional de Promoción Científica y Tecnológica (PICT 20545), CONICET (PIP 5799), Universidad de Buenos Aires (X24), and Instituto Nacional de Tecnología Agropecuaria (INTA).

JF800541F